PROCEEDINGS OF SPIE

Management of all three phases of wound healing through the induction of fluorescence biomodulation using fluorescence light energy

Giovanni Scapagnini, Andrea Marchegiani, Giacomo Rossi, Michela Zago, Joanna Jowarska, et al.

Management of all three phases of wound healing through the induction of fluorescence biomodulation using fluorescence light energy

Giovanni Scapagnini[a,c], Andrea Marchegiani[b], Giacomo Rossi[b], Michela Zago[c], Joanna Jowarska[c], Mohamed Wael[c], Shannon E. Campbell[c], Zachary Schiffman[e,f], Emanuela Buonamici[c], Ricardo Garvao[c], Remigio Piergallini[c], Matteo Cerquetella[b], Alessandro Fruganti[b], Fabrizio Dini[b], Fulvio Laus[b], Andrea Spaterna[b]

a. Department of Medicine and Health Science, University of Molise, Italy; b. School of Biosciences and Veterinary Medicine, University of Camerino, Italy; c. Klox Technologies, Inc., Laval, Quebec, Canada; e. Special Pathogens Program, National Microbiology Laboratory, Public Health Agency of Canada, Winnipeg, Manitoba, Canada; f. Department of Medical Microbiology and Infectious Diseases, University of Manitoba, Winnipeg, Manitoba, Canada

ABSTRACT

Research on photobiomodulation (PBM) has led to the development of various light-generating devices that can benefit a wide range of clinical indications. A novel approach of inducing PBM is through application of a Fluorescence Biomodulation (FB) System consisting of a blue light (peak wavelength between 440 and 460 nm) which activates topical photoconverter substrates containing specialized chromophores that generate fluorescence light energy (FLE). In clinical trials, FLE has been shown to modulate both healthy and disease-affected skin/soft tissue, providing a unique method for managing inflammatory skin conditions and accelerating healing. To better understand the biological impact of FB-induced FLE, we studied this system *in vitro* on dermal human fibroblasts (DHFs) and *in vivo* in canine deep pyoderma.

In vitro data from stimulated DHFs exposed to an FB System showed a significant decrease in IL-6 production by 130.14% after 24 hr ($p<0.001$), compared to control groups. In canines with chronic deep pyoderma, the use of FB plus standard of care (SOC) treatment significantly reduced time to clinical resolution compared to controls that received SOC alone ($p<0.001$). Biopsies from lesional areas showed enhanced mitochondrial biogenesis in the FB lesions versus the SOC lesions, as supported by a significant increase in the number and size of mitochondria (89.31% and 90.15% respectively; $p<0.0001$). Significant modulation of inflammatory pathways, epithelialization, and angiogenesis were also demonstrated.

These results support the use of FB Systems for skin conditions impacted by inflammation and offer a promising therapeutic solution to support its use in other medical conditions.

Keywords: Tissue healing, fluorescence biomodulation, photobiomodulation, acute and chronic wounds, inflammation, angiogenesis, epithelization, remodeling, mitochondria, Stokes shift, skin, soft tissue, ulcers

1. INTRODUCTION

Photobiomodulation (PBM) is widely used for its therapeutic benefits in the protection and regeneration of tissues(1-6). Studies have demonstrated that PBM can reduce pain and inflammation(6-8), improve cancer management(9), and stimulate healing and tissue repair(3-5, 10-14). PBM describes the use of visible light to stimulate biological functions in a non-thermal and non-cytotoxic manner. Advances in understanding how PBM achieves its biological impact have identified endogenous chromophores that are widely expressed in different cells types, including skin cells, as well as in the extracellular matrix. Interactions between light and these chromophores have been demonstrated to modulate biological processes, including inflammation, angiogenesis, and signal transduction pathways that recruit transcription factors activating several genes involved in multiple aspects of cell biology(15).

Although there is still research to be done to further understand the mechanism of action of PBM, studies have identified several key pathways. First, PBM has been demonstrated to directly activate endogenous chromophores (also known as non-visual photoreceptors). Specific examples include cytochrome C oxidase (CCO), a small hemeprotein that is associated with the mitochondria inner membrane and that is sensitive to red and NIR (~610-950 nm) light[16]; flavins, a family of cryptochrome proteins that are involved in the repair of DNA and that are sensitive to blue (~410-500 nm) light[17]; and opsins, a family of proteins that are able to modulate calcium channels, thereby impacting intra-cellular calcium levels and that respond to blue and green (~410-550 nm) light[18]. Another biological pathway modulated by PBM is inflammation. Both *in vitro* and *in vivo* studies have demonstrated the anti-inflammatory action of red (610-760 nm) light through the modulation of interleukin (IL)-1α and β, IL-6, IL-17, and tissue necrosis factor (TNF)-α (7, 19). Additionally, decreases in serum IL-8 and TNFα have also been observed clinically following PBM therapy[8]. Finally, PBM has been demonstrated to help manage oxidative stress, especially in damaged and inflamed tissue(20, 21). Recent work suggests this may be modulated through matrix proteins such as matrix metalloproteinases (MMPs) and their tissue inhibitors[22]. Each of these pathways is implicated in the three phases of healing (inflammation, proliferation, and remodeling), providing clear evidence to support the efficacy of PBM in stimulating wound healing.

Fluorescence biomodulation (FB), a form of PBM that uniquely employs fluorescence light energy (FLE), has been demonstrated to advance healing of both acute and chronic wounds(5, 12-14, 23). Studies have demonstrated that acute incisional wounds have reduced inflammation, as well as more physiologic re-epithelization and collagen remodeling, resulting in better quality and less visible scars(4, 12), and that patients with hard-to-heal chronic ulcers experienced accelerated healing and improved quality of life[5]. Additionally, these studies have documented the safety and efficacy of FB Systems in a variety of impaired skin conditions. FB Systems consist of two components: a light source comprised of blue light emitting diodes (LEDs; peak wavelength between 440 and 460 nm) and a topical photoconverter substrate embedded with chromophores. These FB substrates are constructs, generally of silicone- or nylon-based membranes or amorphous hydrogels, optimized for different therapeutic uses and delivery of photonic energy (Section 2.3 provides more details). Of note, the substrates themselves are not absorbed by the tissue[13, 34], their impact is achieved through the light energy delivered to the tissue. Figure 1 illustrates how the FB substrates absorb photonic energy from the FB lamp and, through a phenomenon known as Stokes shift, subsequently emit energy in the form of FLE that penetrates tissues.
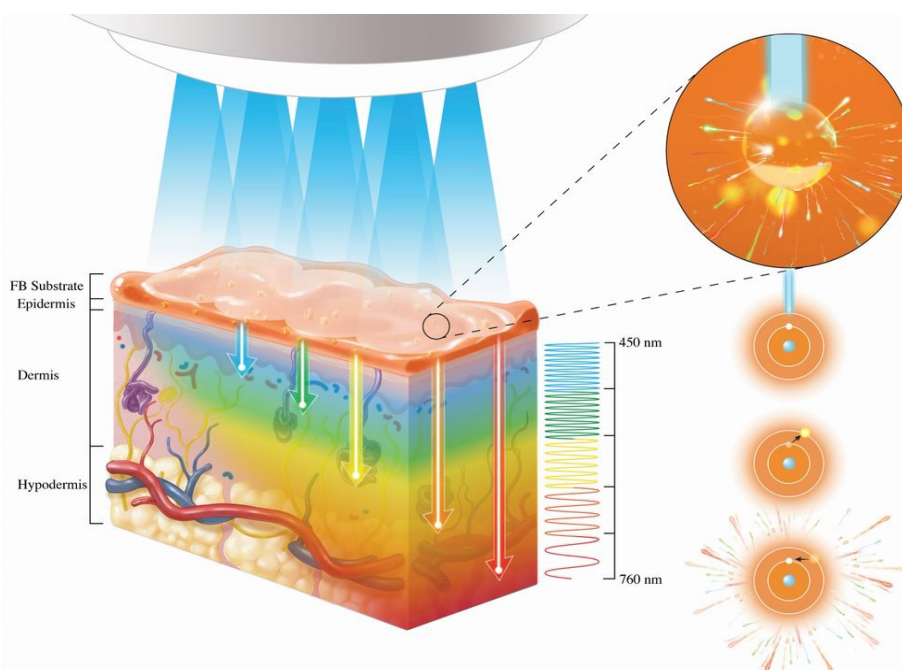

Figure 1. Wavelength dictates the depth of penetration into skin. In FB Systems chromophores embedded within the FB substrate are activated by the FB lamp. The activated chromophores subsequently emit energy in the form of fluorescence

light energy (FLE) though a Stokes shift (illustrated on right side of figure). FLE penetrate skin to different depths depending on the spectral profile emitted. Image created by Klox Technologies Inc.

FB Systems provide both blue light directly from the FB lamp (~400-500 nm) as well as chromophore-generated FLE (~500-760 nm) to the tissue, creating a tunable light signature depending on the substrate that is used. Figure 2 provides some examples of the radiant fluence generated by different FB Systems and delivered to the tissue. In skin different endogenous chromophores have different scattering and absorption coefficients that are highly wavelength-dependent(15). Thus, wavelength of light is widely considered the most important parameter in phototherapy, as it dictates not only which endogenous chromophores are activated but also the depth of penetration into the skin, thereby controlling what part of the tissue is stimulated. Blue to green light penetrates only 1-2.5 mm into the skin, targeting only the epidermis and the top layer of the dermis, whereas red light can penetrate almost 5 mm into the skin, penetrating deep into the dermis and possibly the hypodermis depending on skin thickness(24). FB Systems are unique in delivering incident fluence to tissue both directly from an LED and indirectly as FLE from an activated FB substrate.
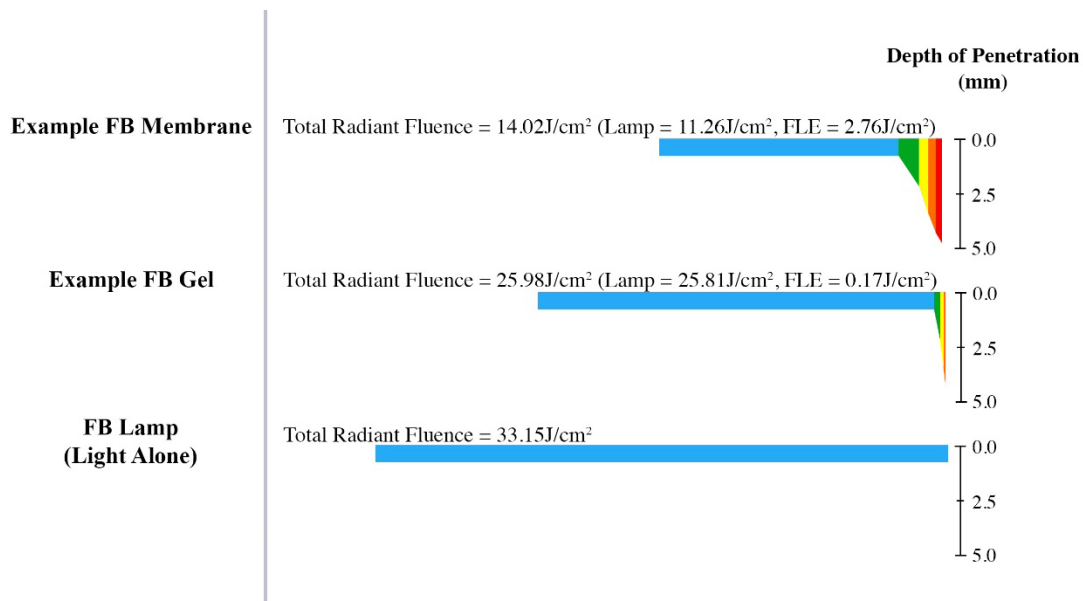

Figure 2. Illustrative example of the light profile delivered by different FB Systems, including the direct radiant fluence from the FB lamp (blue bars), as well as the FLE (colored bars) generated by the FB substrates. Each FB substrate provides a unique spectral profile to the tissue with a distinctive tissue penetration. Image created by Klox Technologies Inc.

In the present studies, we examined whether FLE delivered by FB Systems can stimulate cellular and/or healing responses. *In vitro* models used primary human dermal fibroblast (DHF) cells from the dermal layer of the skin; these cells are involved in the healing response. To confirm findings from *in vitro* models, a pilot study of canine deep pyoderma (CDP) investigated the impact of FB Systems on the healing of chronic lesions. CDP was selected because it is one of the most challenging skin diseases in small animal practice(25, 26), involving severe inflammation and dissemination of bacteria into the deep dermis, sometimes affecting as deeply as the fatty layer beneath the skin(27, 28).

2. MATERIAL AND METHODS

2.1 Fluorescence biomodulation systems

Fluorescence Biomodulation Systems consist of an FB lamp and a topical FB substrate that has a thickness of 1-2 mm (see Figure 3). The FB lamp is a multi-LED light source that delivers non-coherent blue light with a single peak wavelength between 440 and 460 nm. The irradiance or power density is between 110 and 150 mW/cm^2 at 5 cm. FB substrates contain chromophores embedded in a medium appropriate for different therapeutic applications. Substrates used in these studies include silicone-based membranes, nylon-based fibers constructed into membranes, or Carbopol®-based amorphous hydrogels. FB substrates are photoconverters that absorb some of the light from the FB lamp and, through a Stokes shift in the activated chromophore, emit FLE in the range of 500-760 nm.

In these study, five different FB substrates were used, each delivering a unique spectrum of radiant fluence to the cells or tissue. FB Systems were provided by Klox Technologies Inc. (QC, Canada). *In vitro* experiments assessed four different substrates, three membrane-based systems (FB-MEM) and one amorphous hydrogel-based system (FB-GEL). The fifth FB System (FB-GELB) was developed and optimized for use in veterinary applications, and was used only in the CDP study. Amorphous hydrogel-based substrates are packaged in two separate jars, one for the chromophore gel and the other for the carrier gel. Prior to use, the gels are mixed per manufacturers instruction into a single FB substrate ready for illumination. For all *in vitro* experiments, the FB substrates were placed under the slide (not in direct contact with cells), and illumination was conducted through the glass bottom slide with the FB lamp. The glass bottom slide was tested to ensure that no alteration in radiant fluence could be detected.

FB Lamp · FB Membrane · FB Membrane Illuminated by FB Lamp

FB Gel (Chromophore + Carrier) · FB Gel (Mixed) · FB Gel Illuminated by FB Lamp
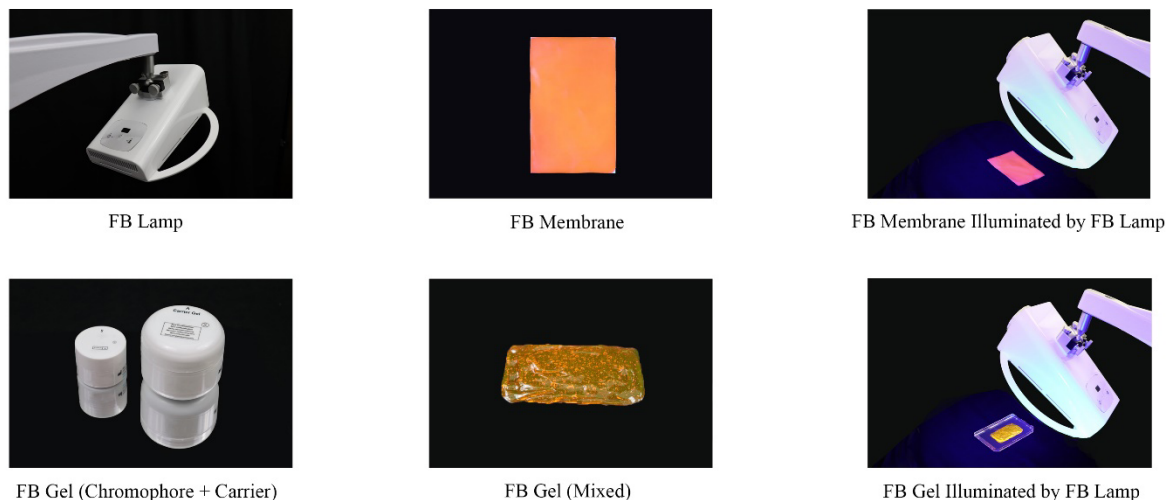
Figure 3. Examples of the FB lamp and different FB substrates. FB substrates (membranes and gels) are illuminated by the FB lamp at a distance of 5 cm. Image created by Klox Technologies Inc.

Table 1 provides an overview of each of the Control and FB groups used in the different studies. The radiant fluences delivered to the cells or tissue by the FB devices tissue during a single illumination are between 12 and 38 J/cm^2, including both direct light from the FB lamp as well as FLE emitted by the FB substrates. Except for FB-GELB, a standard protocol with each FB substrate consists of 5 min of illumination with the FB lamp at approximately 5 cm (per the instructions for use). To determine a dose response to FB substrates were illuminated for shorter or longer periods than 5 min. Additionally, in the CPD study the substrate FB-GELB was illuminated for only 2 min, due to optimization of the procedure for animal care. This protocol still produced sufficient FLE (between 15 and 20 J/cm^2) to trigger biological effects. Any changes from the standard 5 min illumination protocol are noted in the relevant section and on any figures or tables.

Table 1. Overview of acronyms used to describe Control and FB groups. #Lamp alone control cells were illuminated with the FB lamp (no substrate); ¶ Placebo control cells were illuminated with the FB lamp and a placebo substrate (no photoconverters); § Stimulated control cells were pre-treated with a pro-inflammatory cytokine cocktail to simulate an inflamed state.

CONTROL GROUPS		FLUORESCENCE BIOMODULATION GROUPS (illuminated by FB lamp)	
CTRL	Control Non-Illuminated DHF Cells	FB-MEMA	Silicone-based FB Substrate A (Membrane A)
CTLA	Control DHF Cells Illuminated with Lamp Alone[#]	FB-MEMB	Silicone-based FB Substrate B (Membrane B)
CTPL	Control Placebo[¶] Illuminated Cells	FB-MEMC	Nylon-based FB Substrate (Membrane C)
CTST	Control Stimulated[§] DHF Cells	FB-GELA	Carbopol-based Hydrogel FB Substrate A (Gel A)
CSOC	Control Animals treated with Standard of Care	FB-GELB	Carbopol-based Hydrogel FB Substrate B (Gel B)

2.2 *In Vitro* Experiments: Cell culture of human dermal fibroblasts

Normal human dermal fibroblast (DHF) cultures were purchased from American Type Culture Collection (ATCC #PCS-201-012, Manassas, VA, USA). Cells were cultured at 37°C and 5% CO_2 in fibroblast basal medium phenol red-free supplemented with Fibroblasts Growth Kit-Low serum (ATCC). Culture process was performed according to the manufacturer's protocol. Cells were seeded according to the assay performed (see Section 2.4 for additional details). All experiments were performed on cell cultures passage 4 or less, in triplicate to verify data reproducibility and accuracy. A cytotoxicity detection kit (LDH, Cedarlane, Burlington, ON, Canada) was used to measure cell stress. Cell viability was assessed by the CyQUANT Direct Cell Proliferation test and the XTT (2,3-Bis-(2-Methoxy-4-Nitro-5-Sulfophenyl)-2H-Tetrazolium-5-Carboxanilide) cell viability assay (Invitrogen, Waltham, MA, USA).

Preparation of macrophage-conditioned media (MCM): Normal human peripheral blood mononuclear cells (PBMCs; Zen Bio, Durham, NC, USA) were used to isolate monocyte CD14+ using microbeads (Human MACs Miltenyi Biotec, Auburn, CA, USA) according to the manufacturer's protocol. To differentiate monocytes into macrophages, CD14+ monocytes (1x106 cells) were seeded on 2-chamber Lab-Tek slides (Thermo Scientific) and stimulated with rhGM-CSF (100 ng/mL; R&D systems) in complete RPMI Media without phenol red (ATCC), supplemented with 10% FBS, 1% Pen/Strep, and 4 mM L-Glutamine (Sigma-Aldrich, Markham, ON, Canada) on day 1 and day 3. On day 4, cells were stimulated with lipopolysaccharide (LPS; 10 ng/mL; Sigma-Aldrich) plus 50 ng/ml recombinant human interferon gamma (rhIFN-γ, R&D Systems, Minneapolis, MN, USA) for another 3 days. The MCM was collected on day 7 and stored at -80°C until use.

2.3 *In Vitro* Experiments: Fluorescence biomodulation protocols
Membrane A: Prior to illumination cells were seeded at a density of 30,000 cells/well in 2-chamber slides. After 5 hr of incubation at 37°C in a humidified 5%CO_2 environment, cells were pre-stimulated with 300U/ml rhIFN-γ for 1 hr to induce an inflammatory state. FB-MEMA was placed under the slide (no contact with cells) and illuminated with the FB lamp. A dose response was performed to determine the optimal FLE dose for managing inflammation. Cells were illuminated for 2.5 min, 5 min, 7 min, and 10 min, always at a distance of 5 cm from the base of the slide. The membrane was removed after illumination, and fresh rhIFN-γ media were added for the duration of the assay. At 24 hr, 48 hr, and 72 hr post-illumination, supernatants were collected for analysis of inflammatory cytokines, growth factors, and collagen production.

Membrane B: Prior to the illumination cells were seeded at a density of 70,000 cells/well in 2-chamber slides for pro-inflammatory cytokines and growth factors release assessment. Prior to illumination cells were pre-stimulated either with MCM overnight, or with 350 U/mL of rhIFN-γ or a 10 ng/mL recombinant human IL-1 alpha and beta (IL-1α/β) cocktail (R&D Systems) for 3 hr. FB-MEMB was then applied to the bottom of the slide (no contact with cells) and illuminated for a standard 5 min illumination protocol. After illumination cells were cultured in fresh media in the presence of either rhIFN-γ or IL-1α/β cocktail or in fresh media only if the cells had been pre-stimulated with MCM. Supernatants were then collected at 2 hr, 6 hr, 24 hr, and 48 hr to determine the release of cytokines, growth factors, and collagen production.

Membrane C: Prior to the illumination DHFs were seeded in 2-chamber slides at a density of 30,000 cells/well. After 5 hr of incubation at 37°C in a humidified 5% CO_2 environment, cells were pre-stimulated with an IL-1α/β cocktail (20 ng/ml) for 18 hr. The next day the medium was replaced with PBS and the cells were exposed to FB-MEMC (no contact with cells) using a standard 5 min illumination protocol. Fresh IL-1α/β medium was then added, and a time course analysis was performed on IL-6 production with supernatant collected at each time point for analysis.

Gel A: Prior to illumination cells were seeded at a density of 40,000 cells/well in 2-chamber slides for pro-inflammatory cytokines release assessment. Cells were pre-stimulated with MCM overnight. In the morning, the medium was replaced by sterile PBS, FB-GELA was applied to the bottom of the slide (no contact with cells), and cells were illuminated with a standard 5 min illumination protocol. After illumination FB-GELA was removed and cells were cultured in fresh medium alone. Supernatants were collected at 6 and 24 hr to determine the release of cytokines from the cells.

2.4 *In Vitro* Experiments: Analysis of mediators of healing from cell culture

Cytokine secretion: Concentrations of TNF-α, IL-6, IL-8, IL-10, TGF-β1, and TGF-β3 were measured in collected supernatants using the Quantikine enzyme-linked immunosorbent assay (ELISA) kit in accordance with the manufacturer's protocol (R&D Systems, Minneapolis, MN, USA). Absorbance at 450 nm was determined using the Synergy HT microplate reader (Biotek, Winooski, VT, USA) and corrected for absorbance at 570 nm.

Cytokine and growth factor protein microarray: RayBioR C-Series human cytokine antibody array C5 and human growth factor antibody array C1 were performed in accordance with the manufacturer's protocol (RayBiotech, Norcross, GA, USA). Proteins were visualized using a biotinylated antibody cocktail with HRP-Streptavidin concentrate followed by enhanced chemiluminescence (ECL). The membrane was imaged using a ChemiDoc™ MP+ System (Bio-Rad Laboratories, Mississauga, ON, Canada). Data were analyzed using Image 1.49P software.

Collagen production: Cell culture supernatant was collected 48 hr and 72 hr post-illumination and assessed for collagen production using a SIRCOL total soluble collagen assay per the manufacturer's protocol (Biocolor, Northern Ireland, UK).

2.5 Canine Deep Pyoderma: Fluorescence biomodulation protocol

To assess the effectiveness of FB Systems in managing highly inflamed wounds, a pilot study investigated healing of CDP in 14 dogs with at least two lesional areas of deep pyoderma or one lesional area large enough to be divided in two areas. In this single-center, non-blinded, non-randomized controlled study, all dogs were treated with systemic antibiotic (oral cefadroxil CEFA-CURE TABS, MSD Animal Health, Milan, Italy), the current SOC for CDP. One lesional area received only SOC (CSOC), and another received SOC plus twice-weekly FB therapy, consisting of FB-GELB illuminated for 2 min by the FB lamp (FB-GELB). CSOC lesions were covered during illumination. No significant differences were detected between the average histological lesion scores between the groups at baseline prior to treatment initiation (see Table 9). Dogs were evaluated weekly until complete clinical resolution (CR), defined as complete absence of lesions. Antibiotic treatment was continued for two weeks after complete CR for all dogs in the study. Skin biopsies were taken from CSOC and FB-GELB areas at the time of enrolment prior to any treatment (T0) and upon CR of CDP for histomorphological, immunohistochemical, and mitochondrial analysis.

2.6 Canine Deep Pyoderma: Analysis of mediators of healing

Skin biopsies of both the CSOC and FB-GELB lesions were taken from the peripheral region of each lesion prior to treatment (T0) and at the time of CR of all CDP (T1). Animals received subcutaneous block anaesthesia, performed with 2% lidocaine hydrochloride without vasoconstrictor around the site to be biopsied.

Histomorphological analysis: Biopsies were fixed in buffered formalin for light microscopic evaluation, embedded in paraffin, and sectioned into 3-μm serial sections with a rotary microtome (Leica Biosystems, Wetzlar, Germany). Samples were stained with Haematoxylin and Eosin (H&E) and Masson's Trichrome stain (MTS) to evaluate morphological alterations of the tissue, collagen deposition, and scar formation.

Immunohistochemical detection: Sections were also assessed by immunohistochemistry using indirect immunoperoxidase. Lesions were scored for expression of epidermal growth factor (EGF; Santa Cruz Biotech, CA, USA), fibroblast growth factors (FGFs), TGF-β (Biorad Labs, Hercules), TNF-α, Collagen (Coll) I and III, Ki67 (Abcam, Cambridge, MA, USA), Factor VIII (FVIII) and Decorin (DCN) (Antibodies online.com, UK). Cells were evaluated using a light microscope (Carl Zeiss, Jena, Germany), a×40 objective, a×10 eyepiece, and a square eyepiece graticule (10×10 squares, having a total area of 62,500 μm^2). Ten appropriate fields were chosen for each biopsy. Results were expressed as IHC positive cells per 62,500 μm^2. For all parameters, cells on the margins of the tissue sections were not considered for evaluation to avoid inflation of positive cell numbers.

Mitochondrial analysis: For mitochondria evaluation a fragment (approximately 0.5x0.5x0.5 tissue cube) from each biopsy was sampled and processed for transmission electron microscope (TEM) evaluation. Each micro-cube was immediately fixed in a 2% glutaraldehyde solution in 0.1 M cacodylate (TAAB Lab Equipment, Berks, UK) buffer, pH 7.4. Cubes were then post-fixed in 1% osmium tetroxide (OsO4, Agar Scientific, Essex, UK) for 1 hr and dehydrated in sequential steps of acetone (25%, 50%, 75%, and 100% twice) prior to impregnation in increasing concentrations (25%,

50%, 75%, and 100% three times) of resin (TAAB Lab Equipment) in acetone over a 24 hr period. Ultrathin sections were examined on a Phillips CM 100 Compustage (FEI) transmission electron microscope, and digital micrographs were captured by an AMT CCD camera (Deben, London, UK). To analyze mitochondrial morphology sections from skin biopsies were photographed at ×19,000 magnification. Dermal fibroblasts containing numerous mitochondria were randomly selected for analysis. For each sample, five to six mitochondria-rich fibroblasts were analyzed, for which at least two micrographs were captured, allowing the analysis. For aspect ratio, a measure of mitochondrial shape was evaluated.

2.8 Statistical analysis

Data were analyzed by the Student's t-test for group comparisons of normally distributed variables. Values are presented as mean ± standard deviation (SD). If comparison occurred across multiple groups and/or time points, analysis of variance (ANOVA) was performed with Sidak's multiple comparison test. A p-value ≤0.05 was considered statistically significant.

3. RESULTS

3.1 Effects of fluorescence biomodulation on inflammation

The cascade of normal healing occurs in three overlapping phases: inflammatory, proliferative, and remodeling phases. Each of these phases has different key biological mediators that impact the progress of healing (see Figure 4).
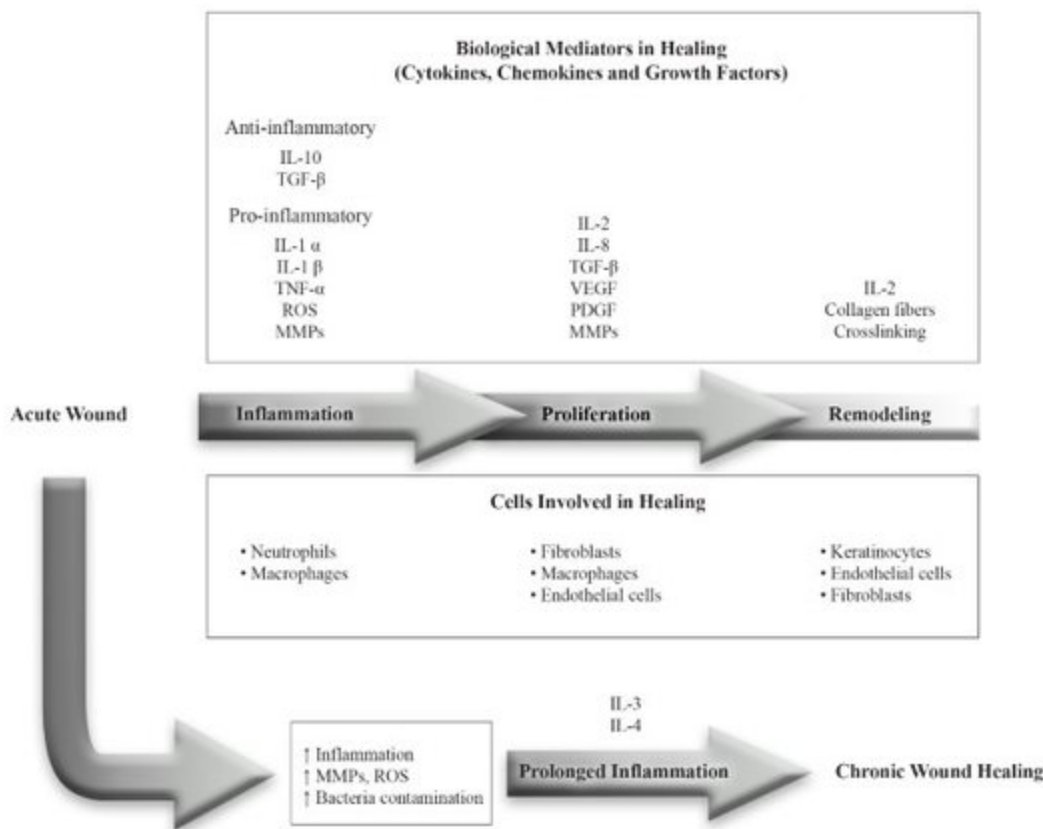

Figure 4. Overview of key mediators and cells involved in the phases of healing. Image created by Klox Technologies Inc.

Wounds can sometimes get stuck or stalled, often in the inflammatory phase, resulting in prolonged inflammation that transitions to a chronic wound. This study aimed to understand which mediators from the different phases of healing may be impacted by FB Systems.

Table 2. Dose response of inflammatory mediators in stimulated DHF cells at 24 hr post-illumination with FB-Mema.

	7 J/cm^2 (2.5 min)	14.4 J/cm^2 (5 min)	19.5 J/cm^2 (7 min)	24 J/cm^2 (10 min)
Increase in FB-MEMA Compared with CTPL	IL-3, IL-8, IL-10, TNF-α, TNF-β, MCP-2, GRO	IL-8, IL-10, MCP-2, GRO	IL-8, IL-10	MCP-1
Decrease in FB-MEMA Compared with CTPL		IL1-α, IL1-β, IL-4, IL-6, TNF-α, TNF-β,	IL1-α, IL1-β, IL-3, IL-4, IL-6, TNF-α, TNF-β, MCP-2, MCP-3, M-CSF, ENA-78, TARC, RANTES, MIP1-Δ	IL1-α, IL1-β, IL-4, IL-6, IL-8, TNF-α, TNF-β, INF-γ, MCP-2, MCP-3, M-CSF, ENA-78, TARC, RANTES, MIP1-Δ

Dose response analysis (Table 2) of FB using FB-MEMA demonstrated that duration of illumination impacted the inflammatory response in DHFs at 24 hr post-illumination.

Table 3. Inflammatory mediators in stimulated DHF cells to 7 min (19.5 J/cm^2) at 48 hr and 72 hr post-illumination.

	48 hr	72 hr
Increase in FB-MEMA Compared with CTPL	IL-2	IL-2
Decrease in FB-MEMA Compared with CTPL	IL1-α, IL1-β, IL-4, IL-5, IL-6, IL-12p40/70, TNF-α, TNF-β, INF-γ	IL1-α, IL1-β, IL-4, IL-5, IL-6, IL-12p40/70, TNF-α, TNF-β, INF-γ

Protein microarrays of cytokines and growth factors provided insights into the inflammatory mediators most impacted by FLE for 2.5 min, 5 min, 7 min, and 10 min, enabling the selection of 5 or 7 min as the optimal duration of illumination for FB-MEMA. Further analysis of the impact of 7 min of FLE with FB-MEMB in Table 3 demonstrated a sustained ability to reduce pro-inflammatory cytokines (IL-6, TNF-α, and IL-4) at 48 hr and 72 hr post-illumination. Of note, IL-8 and IL-10 were elevated at 24 hr (Table 2) and IL-2 was elevated at 48 hr and 72 hr post-illumination (Table 3) relative to placebo illuminated controls, while IL-1 and TNF-α, TNF-β and INF-γ were decreased, suggesting FB would positively impact healing by reducing inflammation and promoting angiogenesis. Additionally, key growth factors (Table 4) for the proliferation/remodeling were also increased at 48 hr and 72 hr after a 7 min illumination.

Table 4. Up-regulated growth factor at 48 hr and 72 hr post-illumination with FB-MEMA compared with Placebo (CTPL).

Time Post-Illumination	14.4 J/cm^2 (5 min)	19.5 J/cm^2 (7 min)	24 J/cm^2 (10 min)
48 hr	No significant changes relative to control CTPL	TGF-β1, TGF-β2, bFGF, PDGF AA, PDGF BB, IGFBP-4, IGF-2, M-CSF, Areg, bNGF, HB, HGF, VGF R3	IGFBP-6, IGF-2, M-CSF, M-CSFR, G-CSR, GM-CSF, Areg, bFGF, bNGF, EGF, FGF-4, HB
72 hr	No significant changes relative to CTPL	TGF-β2, TGF-β3, bFGF, FGF-6, EGFR, EGF, VEGF, VEGF R2, VEGF D, VGF R3, PLGF, PDGF Rα, PDGF AA, PDGF BB, IGFBP-1-4, IGF-1, IGFI-sR, NT4, bNGF, HB	TGF-α, TGF-β2, TGF-β3, bFGF, EGF, HGF, VEGF, VEGF R2, VEGF R3, VEGF D, PFGF AA, PDGF BB, PLGF, IGFBP-1-4, IGF2, NT3, NT4, SCF R, bNGF, GDNF, HB

FB-MEMB, an FB substrate that emits more green FLE (500-570 nm, ~0.97 J/cm^2) than FB-MEMA (500-570 nm, ~0.14 J/cm^2), was compared with control cells illuminated with a placebo substrate for 5 min (CTPL). Results in Table 5 demonstrated that 24 hr post-illumination, all cells had elevated IL-1β and the growth factors RANTES and FGF-7 and a decreased TNF-α, however FB-MEMB also increased proliferative the growth factors TGF-β3, EGF, and PDGF which support proliferation and maturation.

Table 5. Inflammatory profiles on IL-1α/β-stimulated DHF at 24 hr post-illumination with either placebo (CTPL) or FB-MEMB cells compared with non-illuminated stimulated controls (CTST).

	CTPL	FB-MEM B
Increase in FB-MEMB Compared with CTST	IL-1α, IL-1β, RANTES, FGF-7	IL-1α, IL-1β, IL-6, TGF-β1, TGF-β3, TNF-β, RANTES, EGF, PDGFBB, FGF-7, FGF-9, IGFBP-1, IGFBP-4, PLGF
Decrease in FB-MEMB Compared with CTST	TNF-α, EGF-4, IGFBP-4, PLGF	IL-10, TNF-α, FGF-4

Of note, Figure 5 reports that FB-GELA, a completely different FB substrate with a very different radiant fluence profile (12–18 J/cm^2), is also able to decrease the pro-inflammatory cytokines IL-6 and TNF-α compared with both blank and

placebo control. TNF-α release was decreased at an early stage of the inflammation (6 hr) when DHFs were compared to cells stimulated with MCM only and also when compared to the placebo with the illumination group.
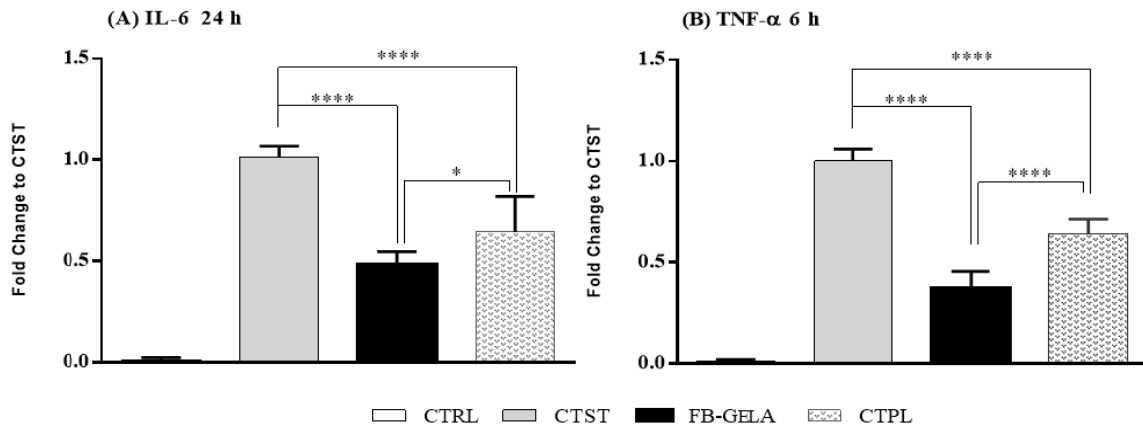

Figure 5. Response of inflammatory mediators at 6 hr (A) and 24 hr (B) post-illumination. Data are expressed as mean ±SD; *p<0.05, ***p<0.001, ****p<0.0001.

Often considered a late-production cytokine, IL-6 release was observed only after 48 hr and was significantly reduced by FB compared with placebo control (CTPL). It is interesting that while this amorphous hydrogel-based FB substrate has such a small FLE profile, its biological impact is still statistically different from lamp alone controls. A very similar anti-inflammatory profile is obtained with FB-MEMC with a decrease in IL-6 from 3 hr to 24 hr post-illumination compared with stimulated control cells. At 48 hr and 72 hr post-illumination IL-6 release gradually returned to baseline (Figure 6).
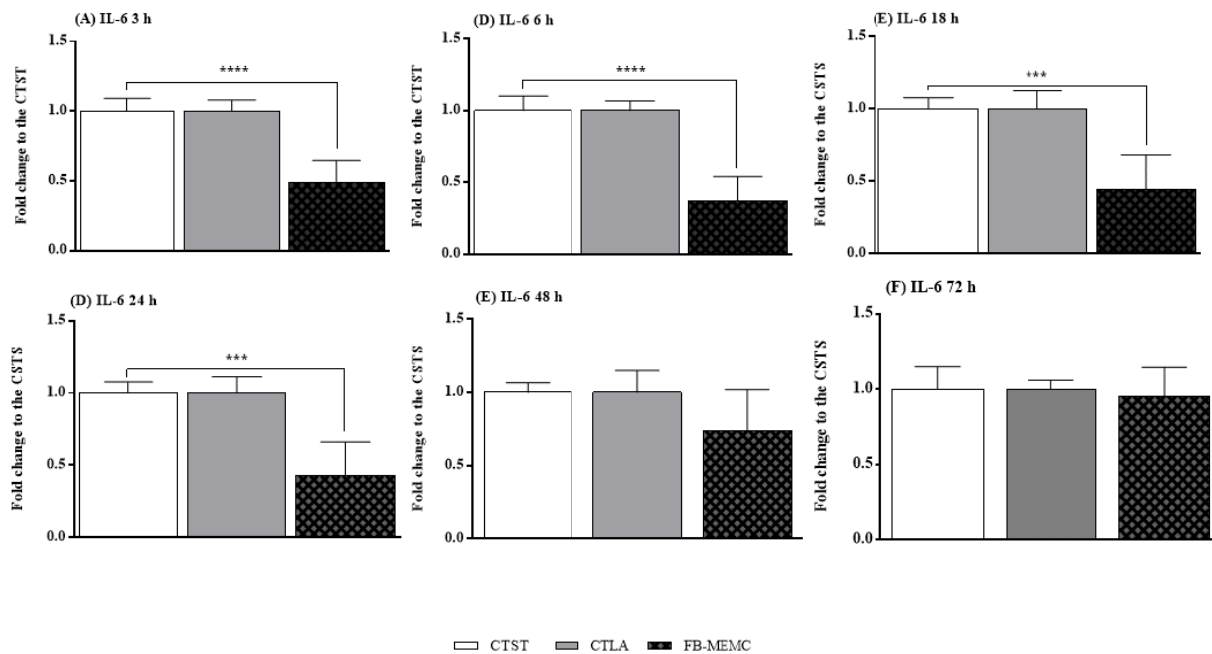

Figure 6. Response of the inflammatory mediator IL-6 in stimulated DHF cells that were non-illuminated (CTST) or illuminated with lamp alone (CTLA) or FB-MEMC at 3 hr (A), 6 hr (B), 18 hr (C), 24 hr (D), 48 hr (E), and 72 hr (F). Data are expressed as mean ±SD; ***p<0.001, ****p<0.0001.

3.2 Effect of fluorescence biomodulation on proliferation

During the proliferation phase of healing the wound is "rebuilt" with new granulation tissue, which is comprised of collagen and extracellular matrix (ECM). Table 6 demonstrates that illumination with FB-MEMA results in confluent cultures after 48 hr that were three-fold higher compared with placebo. Although this difference was not observed at 72 hr, by this time it is likely that growth may have reached a plateau or that the cells could not grow anymore due to the confluence (cell contact inhibition).

Table 6. Cell proliferation expressed as fold increase compared to non-illuminated, stimulated controls (CTST).

Time Post-Illumination	CTST	CTPL	FB-MEMA
24 hr	1	1	1
48 hr	1	1.4	4.82
72 hr	1	1.1	2.99

Nevertheless, a cell viability assay performed on stimulated DHFs exposed to FB-MEMC for up to 72 hr demonstrated a significant increase of the viability ($p<0.0001$; Figure 7), potentially due to an induction of cellular proliferation.
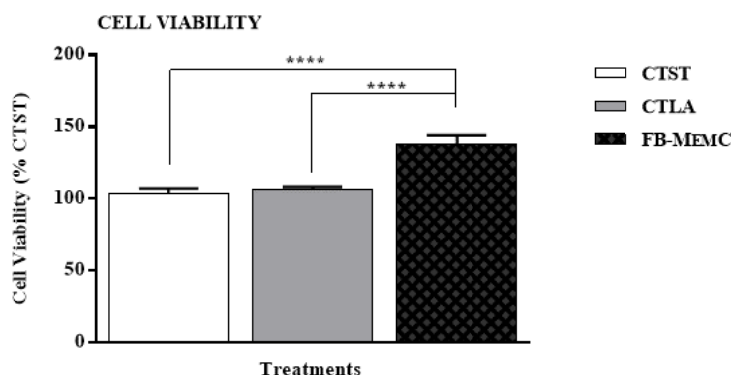

Figure 7. Cell viability of stimulated DHF cells that are non-illuminated (CTST) or illuminated with either lamp alone (CTLA) or FB-MEMC. Data expressed as mean ±SD; ****$p<0.0001$.

3.3 Effect of fluorescence biomodulation of collagen production

Total collagen production analysis revealed that FB-MEMA-illuminated DHF cells produced and secreted six times more collagen then non-illuminated CTRL cells (Table 7). Production and synthesis of collagen is required for the restoration of tensile strength of skin after wound healing.

Table 7. Total collagen (ug/ml) secreted by DHF cells at 48 hr in non-illuminated control cells (CTRL) and cells illuminated with a standard 5 min illumination protocol: placebo (CTPL), lamp alone (CTLA), and FB-MEMA.

Time Post-Illumination	CTRL	CTPL	CTLA	FB-MEMA
48 hr	7.5	12.8	19.9	45.9

Interestingly, Figure 8 presents that FB-MEMB did not alter collagen production 72 hr after a standard 5 min illumination protocol, regardless of stimulation method. This suggests that the radiant fluent profile of FB-MEMB, with more direct blue light (450-500 nm, ~2.93 J/cm^2) and more green FLE (500-570 nm, ~0.97 J/cm^2), can provide a different biological impact than FB-MEMA (450-500 nm, ~3.79 J/cm^2; Green = 500-570 nm, ~0.56 J/cm^2).
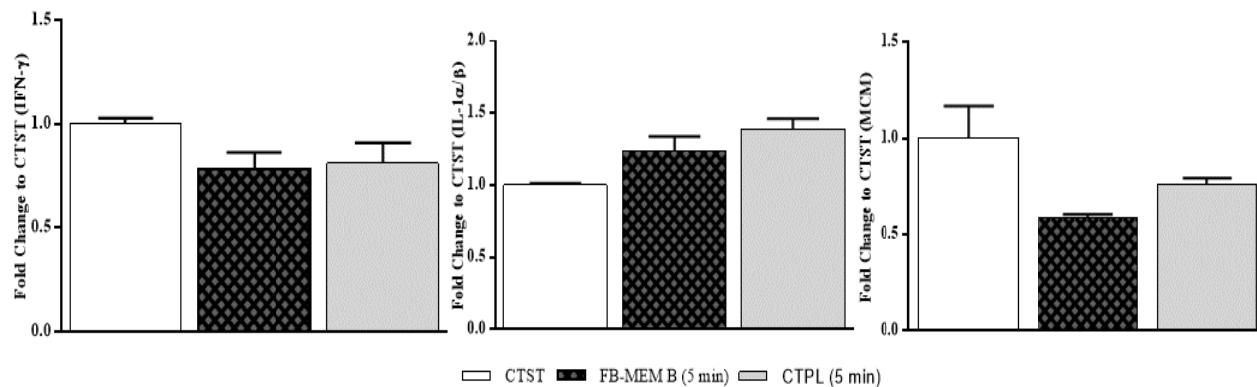
Figure 8. Collagen production in stimulated DHF cells 72 hr post-illumination with FB-MᴇᴍB compared with placebo (CTPL) and non-illuminated, stimulated cells (CTST). No significant differences were detected.

3.4 Effect of fluorescence biomodulation on healing of canine deep pyoderma

In this pilot study of FB Systems use for management of CDP, 100% percent of dogs achieved complete CR irrespective of the protocol administered. No significant differences in sex distribution, age, body weight, number of purebred dogs, and lesion sites were identified. Table 8 demonstrates that there were no significant differences between the control (CSOC) and FB-GᴇʟB average histological lesion scores prior to the commencement of treatment (T0).

Table 8. Average histological lesion scores at baseline (T0) of control (CSOC) and illuminated (FB-GᴇʟB) lesions; Mean (SD).

	TGF-β	TNF-α	F-VIII	FGF	EGF	DCN	Coll III
CSOC	2.53 (3.70)	200.80 (160.13)	28.67 (29.76)	10.53 (7.39)	10.67 (12.98)	6.67 (6.15)	7.33 (5.75)
FB-GᴇʟB	3.27 (3.49)	212.40 (115.37)	27.33 (19.85)	12.40 (7.14)	11.13 (11.59)	5.87 (4.50)	7.20 (4.13)
P-ᴠᴀʟᴜᴇs	0.58	0.82	0.89	0.49	0.92	0.69	0.94

Upon initiation of the pilot study, the clinical conditions of all dogs did not worsen, and no adverse events to antibiotic therapy or FB System exposure were registered by the clinician or reported by the dogs' owners. The combination regimen of cefadroxil and twice-weekly FB-GᴇʟB exhibited an excellent safety profile and achieved CR in 4.3±1.3 weeks (mean±SD, p=0.0001) in all illuminated areas, compared to 7.36±1.61 weeks for CSOC lesions treated with SOC antibiotics alone.

At T1 (4.3±1.3 weeks) histological evaluation showed better quality of tissues from FB-GᴇʟB lesions compared to CSOC lesions, exhibiting less damage and less inflammation of tissues, as well as complete re-epithelialization, a strong neoangiogenesis and the presence of synthesis activities of the connective matrix. These observations were reflected in the histopathological scores, which revealed significant improvement in FB-GᴇʟB-lesions. At T1 the FB-GᴇʟB lesions displayed better epidermal integrity compared to CSOC lesions, which did not always show complete epithelial integrity. Immunostaining for epidermal and fibroblast growth factors (EGFs and FGFs) revealed a constantly strong cellular expression of these two markers in the FB-GᴇʟB lesions compared to CSOC lesions (see Figure 9) for all the parameters evaluated. These data demonstrate that FB-GᴇʟB lesions underwent a qualitatively better re-epithelialization process with a decreased inflammatory status.
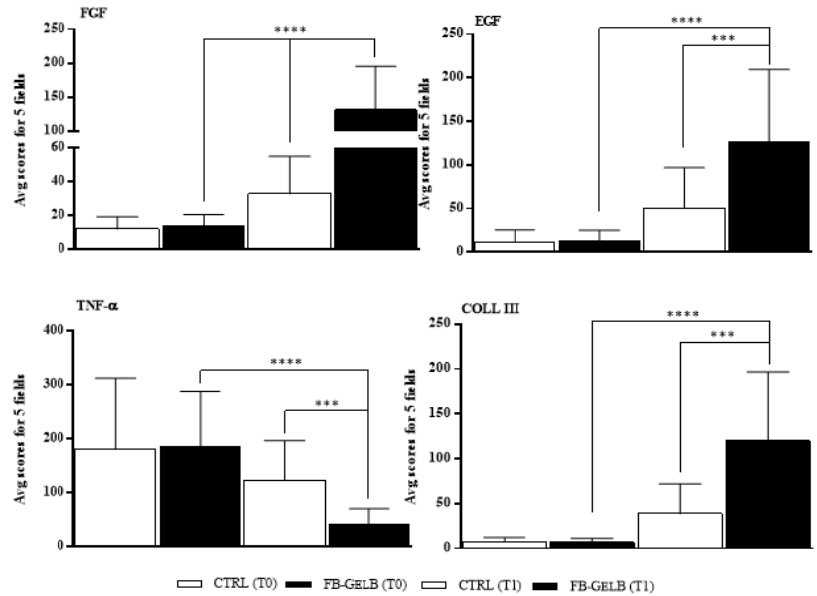
Figure 9. Immunohistochemical markers over time between the CSOC and FB-GELB lesions. Error bars indicate the mean±SD. Data are expressed as mean±SD (***p<0.001, ****p<0.0001).

Of significant interest, this pilot work also suggests that FB impacts mitochondria during healing. Table 9 demonstrates that relative to baseline, lesions from FB-GELB taken at T1 had a 10-fold increase in the size of mitochondria compared with T1 CSOC lesions (90.15% increase vs. 9.09% increase $p < 0.0001$, respectively). Additionally, at T1, mitochondria in the FB-GELB lesions appear more elongated and ovoid, with clearly defined cristae compared with more circular and less defined cristae in samples from both T0 (all lesions) and T1 CSOC lesions. Furthermore, FB-GELB lesions demonstrated a substantial increase (89.31%) in the number of mitochondria from baseline to T1, compared with only a 12.09% increase from T0 to T1 in CSOC lesions ($p < 0.0001$). Figure 10 are representative TEM images of the mitochondria at baseline (T0) and at T1 for CSOC and FB-GELB biopsy samples.

Table 9. Mitochondrial changes from T0 to T1 in CSOC and FB-GELB lesions. ****p<0.0001

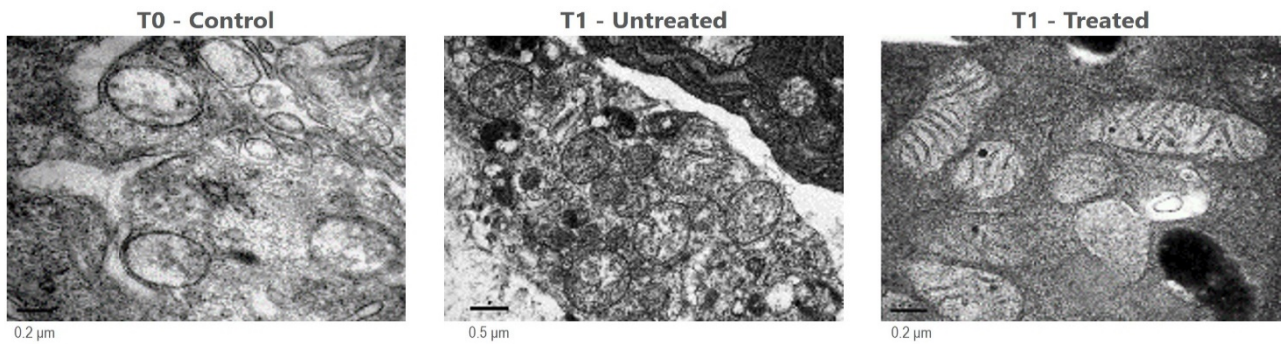| Sample	Time	Number of Mitochondria	Increase in Number from T0	Size (μm)	Increase in Size from T0
CSOC	T0	3.83	12.09%	0.95	9.09%
	T1	4.36		1.04	
FB-GELB	T0	4.26	89.31%****	0.77	90.15%****
	T1	11.12		2.04	

Figure 10. TEM images of mitochondria comparing CSOC baseline (T0) to CSOC and FB-GELB at CR (T1; 4.3±1.3 weeks).

Table 10 provides a summary to compare the inflammatory and growth factor profiles after illumination with FB compared with placebo or SOC controls. Of note, biological mediators in the supernatant of cell cultures treated with all Membranes (A-C), as well as FB-GELA, were assessed *in vitro* 24 hr after illumination with a standard 5 min protocol. FB-MEMA and FB-MEMB were assessed using protein micro-arrays for cytokines and growth factors, and the results for IL-6, TNF-α, and TGF-β3 were further confirmed with ELISA assays. FB-MEMC were assessed with ELISA assays for each mediator tested. Conversely, inflammatory profiles of FB-GELB were assessed in biopsy samples of CDP lesions upon clinical resolution (T1) by immunohistochemistry.

Table 10. Overview of biological mediators impacted by different FB substrates. (NT = Not Tested)

	FB-MEMA	FB-MEMB	FB-MEMC	FB-GELA	FB-GELB
Pro-Inflammatory Cytokines					
IL-1 α	↓	↑	NT	NT	NT
IL-1 β	↓	↑	NT	NT	NT
IL-6	↓	↑	↓	↓	NT
TNF- α	↓	↓	--	↓	↓
Anti-Inflammatory Cytokines					
IL-10	↑	↓	NT	NT	NT
Prolonged Inflammatory Cytokines					
IL-3	↓	NT	NT	NT	NT
IL-4	↓	NT	NT	NT	NT
Proliferative Cytokines					
IL-2	↑	NT	NT	NT	NT
IL-8	↑	NT	NT	NT	NT
Growth Factors					
TGF- β 1	↑	↑	NT	NT	↑
TGF- β 3	↑	↑	NT	NT	NT
VEGF	↑	NT	NT	NT	↑
FGF	↑	↑	NT	NT	↑
PDGF	↑	NT	NT	NT	↑

FB-MEMB provides less total light to the tissue (400-760 nm, ~9.87 J/cm^2) than FB-MEMC (400-760 nm, ~20.99 J/cm^2) and has a much greater fluence in the green wavelengths (500-570 nm, 0.97 J/cm^2 vs. 0.36 J/cm^2, respectively). Both FB substrates increase the anti-inflammatory cytokine IL-10 and decrease the pro-inflammatory cytokine TNF-α. However, FB-MEMA decreases IL-6 and increases collagen, and FB-MEMB impacts TGF-β. Of note, even the small amount of FLE released by the amorphous hydrogel FB substrates (500-760 nn, 0.12-0.21 J/cm^2) are able to induce biological effects, impacting both inflammatory cytokines and growth factors.

4. DISCUSSION

This body of work assessed the impact of a novel technology, fluorescence biomodulation, on biological mediators of inflammation and healing. Dose response studies demonstrated that the optimal chromophore activation duration for improving the inflammatory profile in DHF cells was 5 or 7 min. For ease of use, the 5 min illumination protocol was selected as the optimal time in human clinical settings. Additionally, FLE from both membrane and amorphous hydrogel substrates induced DHFs to positively modulate their inflammatory profiles and up-regulate growth factors, producing environments more conducive to healing. In the CDP study, FB Systems yielded significant biological effects that impacted inflammation, stimulated markers of proliferation and angiogenesis, and improved markers of tissue remodeling, indicating that FB Systems impact all three phases of healing. Both *in vitro* and *in vivo* results demonstrated improved inflammatory profiles, with down-regulation of pro-inflammatory cytokines like IL-6 and TNF-α and up-regulation of anti-inflammatory cytokines like IL-10 and TGF-β3. Additionally, protein microarrays suggest that DHF cells were less likely to produce IL-4, a cytokine that appears to be linked to the pathogenesis of chronic wounds(29, 30). Growth factors such as TGF-β, FGF, PDGF, and VEGF were also elevated by FLE. These growth factors are needed to initiate and support proliferation of new granulation tissue, including angiogenesis to build the vessel networks for blood supply(31-33). The final phase of healing is the remodeling of collagen leading to the full closure of the wound. FB

Systems impact this phase by increasing TGF-β3 and decorin, both of which aid in the final maturation of the new tissue(34, 35).

The FB Systems used in this study consist of the FB lamp and FB substrates (membranes or amorphous hydrogels) with embedded chromophores that absorb some of the light from the FB lamp and emit FLE in the 500-760 nm range. Despite the small amount of FLE, biological effects are detectable *in vitro* and *in vivo*, with enhanced healing of acute and chronic wounds in humans well documented(5, 12-14, 23, 36-38). The delivery of FLE by the FB substrates results in stimulation of more beneficial cellular processes, compared with cells and tissues directly illuminated with a light source alone, even even when the light sources matches the FLE spectra(39). Direct light is known to have biological effects, and the direct delivery of blue light (~450-500 nm) to the cells and tissue from the FB lamp could also be involved in up-regulation of growth factors and/or improved healing, providing a synergistic impact with FLE (~500-760 nm). It is interesting to note that FB-MEMA, which provides more blue light and less green FLE than FB-MEMB, decreased all anti-inflammatory cytokines measures, whereas FB-MEMB only down-regulated TNF-α. FB-MEMB however did not stimulate collagen production, therefore is more appropriate for reducing scarring than accelerating healing in chronic wound. These two FB membranes also impacted IL-10 in an opposite manner. Interestingly, both the membranes and gels were able to stimulate growth factor production, key mediators in the later phases of healing. These data suggest that FLE production, and its biological impact, are tunable and that different FB substrates can be optimized to address different types of acute and chronic skin pathologies.

Studies of PBM have identified several light-sensitive entities in the skin, which generally fall into two categories: non-visible photoreceptors and photoaccepters. Non-visible photoreceptors (sometimes referred to as photosensitizers) are endogenous chromophores that can absorb light within the visible spectrum (400-800 nm) and subsequently re-emit this light with a lower energy and longer wavelength (Stokes shift) in the form of fluorescence (primary) and phosphorescence (secondary)(40). These non-visible photoreceptors are present within the cells of the skin and include proteins such as flavins, NADH, bilirubin, and melanin. Additionally, skin also contains photoacceptors, defined as proteins or protein complexes that do not require light for their activity but can harness light energy to enhance their activity(40). When FB technologies shift light to longer wavelengths resulting in deeper penetration into the tissue, they potentially activate a variety of endogenous chromophores such as flavins/riboflavins, COX IV, and NADH(15, 40, 41). COX IV represents the terminal complex in the electron transport chain that plays a critical role in reducing oxygen to water, contributing to the proton gradient required for subsequent ATP production. It has been proposed that light energy can dissociate nitric oxide from COX IV, thereby increasing its activity; this increases ATP production and alters the cellular redox state(1, 40, 42). Given the preliminary results observed in this study demonstrating the impact of FB on mitochondria size, shape, and number, there is a strong possibility that COX IV is a primary target for the FLEs generated by the different FB substrates. Of note, the lower wavelength (blue-green) light provided by FB Systems could also be contributing to accelerated healing. These wavelengths can excite light-sensitive opsin proteins that open ion-sensitive channels to regulate intracellular calcium(43). Together these light-sensitive pathways can impact reactive oxygen species (ROS), cyclic AMP (cAMP), and numerous transcription factors that can influence protein synthesis, cell migration, collagen and extracellular matrix (ECM) deposition, and proliferation(40, 41, 44-48).

The models selected for this body of work included *in vitro* studies of DHF cells and an *in vivo* study of CPD as a wound healing model. Fibroblasts are the most abundant cell type in the dermal layer of skin; they are also accessory cells in the inflammatory response. Fibroblasts can produce or respond to a wide variety of cytokines, and these mediators allow fibroblasts and leukocytes to cooperate during complex processes such as wound healing. Investigating the effect of DHF cells provides insight into how FB Systems impact each phase of healing. CDP is a challenging chronic inflammatory skin disease associated with severe inflammation(25, 26). It responds poorly to treatment, often requiring long-term oral antibiotic therapy(28). Illumination with FB-GELB in conjunction with SOC antibiotics resulted in earlier CR, indicating that FB Systems accelerate healing, likely through decreasing inflammation and improving mitochondrial function. These preliminary results demonstrate for the first time that tissues exposed to FB Systems showed an active mitochondrial biogenesis, characterized by the growth and division of preexisting mitochondria. This phenomenon is not only accompanied by increased mitochondria numbers but also by an increase in their size. Pathologic conditions of

tissues, primarily aging and degenerative or inflammatory processes, are intimately associated with the decline in mitochondrial number and functionality. Furthermore, mitochondrial disfunction has been directly associated with the inability of proinflammatory M1 macrophages to reprogramming to a more homeostatic M2 phenotype, creating a metabolic roadblock in the resolution of inflammatory process, as typically observed in chronic wound(49). In recent years, a growing number of papers have theorized that mitochondrial number, size, and function determine tissue health and longevity(50-52).

In conclusion, this study indicates that FB Systems, already used in human health to manage acne vulgaris, rosacea, and many types of ulcers(5, 12-14, 23, 36-38), positively impact all phases of healing through modulation of the inflammatory profile, activation of growth factors, and stimulation of collagen depositions in a physiological manner. This provides mechanistic evidence that aligns with the accelerated healing and improved clinical outcomes observed *in vivo* in this study, as well as in patients in clinical settings(5).

5. ACKNOWLEDGMENTS

REFERENCES

[1] P. Avci, A. Gupta, M. Sadasivam *et al.*, "Low-level laser (light) therapy (LLLT) in skin: stimulating, healing, restoring," Semin Cutan Med Surg*, 32(1), 41-52 (2013).

[2] M. R. Hamblin, "Photobiomodulation or low-level laser therapy," J Biophotonics*, 9(11-12), 1122-1124 (2016).

[3] S. Kulkarni, M. Meer, and R. George, "Efficacy of photobiomodulation on accelerating bone healing after tooth extraction: a systematic review," Lasers Med Sci, (2018).

[4] R. M. Ramos, M. Burland, J. B. Silva *et al.*, "Photobiomodulation Improved the First Stages of Wound Healing Process After Abdominoplasty: An Experimental, Double-Blinded, Non-randomized Clinical Trial," Aesthetic Plast Surg, (2018).

[5] M. Romanelli, A. Piaggesi, G. Scapagnini *et al.*, "Evaluation of fluorescence biomodulation in the real-life management of chronic wounds: the EUREKA trial," J Wound Care*, 27(11), 744-753 (2018).

[6] M. Traverzim, S. Makabe, D. F. T. Silva *et al.*, "Effect of led photobiomodulation on analgesia during labor: Study protocol for a randomized clinical trial," Medicine (Baltimore)*, 97(25), e11120 (2018).

[7] M. da-Palma-Cruz, R. F. da Silva, D. Monteiro *et al.*, "Photobiomodulation modulates the resolution of inflammation during acute lung injury induced by sepsis," Lasers Med Sci, (2018).

[8] L. G. Langella, H. L. Casalechi, S. S. Tomazoni *et al.*, "Photobiomodulation therapy (PBMT) on acute pain and inflammation in patients who underwent total hip arthroplasty-a randomized, triple-blind, placebo-controlled clinical trial," Lasers Med Sci, (2018).

[9] G. D. Baxter, L. Liu, S. Petrich *et al.*, "Low level laser therapy (Photobiomodulation therapy) for breast cancer-related lymphedema: a systematic review," BMC Cancer*, 17(1), 833 (2017).

[10] M. R. Hamblin, "Photobiomodulation, photomedicine, and laser surgery: a new leap forward into the light for the 21(st) century," Photomed Laser Surg*, 36(8), 395-396 (2018).

[11] D. P. Kuffler, "Photobiomodulation in promoting wound healing: a review," Regen Med*, 11(1), 107-22 (2016).

[12] T. Fogacci, F. Cattin, G. Semprini *et al.*, "The use of chromophore gel-assisted blue light phototherapy (Lumiheal) for the treatment of surgical site infections in breast surgery," Breast J*, 24(6), 1135 (2018).

[13] A. Nikolis, S. Bernstein, B. Kinney *et al.*, "A randomized, placebo-controlled, single-blinded, split-faced clinical trial evaluating the efficacy and safety of KLOX-001 gel formulation with KLOX light-emitting diode light on facial rejuvenation," Clin Cosmet Investig Dermatol*, 9, 115-25 (2016).

[14] A. Nikolis, D. Grimard, Y. Pesant *et al.*, "A prospective case series evaluating the safety and efficacy of the Klox BioPhotonic System in venous leg ulcers," Chronic Wound Care Magement and Research*, 3, 101—111 (2016).

[15] L. F. de Freitas, and M. R. Hamblin, "Proposed mechanisms of photobiomodulation or low-level light Therapy," IEEE J Sel Top Quantum Electron*, 22(3), (2016).

[16] T. I. Karu, "Multiple roles of cytochrome c oxidase in mammalian cells under action of red and IR-A radiation," IUBMB Life, 62(8), 607-10 (2010).

[17] A. Becker, A. Klapczynski, N. Kuch *et al.*, "Gene expression profiling reveals aryl hydrocarbon receptor as a possible target for photobiomodulation when using blue light," Sci Rep, 6, 33847 (2016).

[18] Y. Wang, Y. Y. Huang, Y. Wang *et al.*, "Photobiomodulation (blue and green light) encourages osteoblastic-differentiation of human adipose-derived stem cells: role of intracellular calcium and light-gated ion channels," Sci Rep, 6, 33719 (2016).

[19] W. H. Li, A. Fassih, C. Binner *et al.*, "Low-level red LED light inhibits hyperkeratinization and inflammation induced by unsaturated fatty acid in an in vitro model mimicking acne," Lasers Surg Med, 50(2), 158-165 (2018).

[20] S. A. Dos Santos, M. A. Dos Santos Vieira, M. C. B. Simoes *et al.*, "Photobiomodulation therapy associated with treadmill training in the oxidative stress in a collagen-induced arthritis model," Lasers Med Sci, 32(5), 1071-1079 (2017).

[21] J. C. Tatmatsu-Rocha, C. Ferraresi, M. R. Hamblin *et al.*, "Low-level laser therapy (904nm) can increase collagen and reduce oxidative and nitrosative stress in diabetic wounded mouse skin," J Photochem Photobiol B, 164, 96-102 (2016).

[22] S. M. Ayuk, H. Abrahamse, and N. N. Houreld, "Photobiomodulation alters matrix protein activity in stressed fibroblast cells in vitro," J Biophotonics, 11(3), (2018).

[23] M. Sannino, G. Lodi, M. W. Dethlefsen *et al.*, "Fluorescent light energy: Treating rosacea subtypes 1, 2, and 3," Clin Case Rep, 6(12), 2385-2390 (2018).

[24] C. Ash, M. Dubec, K. Donne *et al.*, "Effect of wavelength and beam width on penetration in light-tissue interaction using computational methods," Lasers Med Sci, 32(8), 1909-1918 (2017).

[25] E. M. Lund, P. J. Armstrong, C. A. Kirk *et al.*, "Health status and population characteristics of dogs and cats examined at private veterinary practices in the United States," J Am Vet Med Assoc, 214(9), 1336-41 (1999).

[26] G. Rossi, M. Cerquetella, and A. R. Attili, "Amphixenosic Aspects of Staphylococcus aureus Infection in Man and Animals," Curr Top Microbiol Immunol, 409, 297-323 (2017).

[27] L. A. Devriese, M. Vancanneyt, M. Baele *et al.*, "Staphylococcus pseudintermedius sp. nov., a coagulase-positive species from animals," Int J Syst Evol Microbiol, 55(Pt 4), 1569-73 (2005).

[28] J. R. Fitzgerald, "The Staphylococcus intermedius group of bacterial pathogens: species re-classification, pathogenesis and the emergence of meticillin resistance," Vet Dermatol, 20(5-6), 490-5 (2009).

[29] A. P. M. Serezani, G. Bozdogan, S. Sehra *et al.*, "IL-4 impairs wound healing potential in the skin by repressing fibronectin expression," J Allergy Clin Immunol, 139(1), 142-151 e5 (2017).

[30] T. A. Wynn, "Type 2 cytokines: mechanisms and therapeutic strategies," Nat Rev Immunol, 15(5), 271-82 (2015).

[31] S. Barrientos, O. Stojadinovic, M. S. Golinko *et al.*, "Growth factors and cytokines in wound healing," Wound Repair Regen, 16(5), 585-601 (2008).

[32] B. Behm, P. Babilas, M. Landthaler *et al.*, "Cytokines, chemokines and growth factors in wound healing," J Eur Acad Dermatol Venereol, 26(7), 812-20 (2012).

[33] S. Werner, H. Smola, X. Liao *et al.*, "The function of KGF in morphogenesis of epithelium and reepithelialization of wounds," Science, 266(5186), 819-22 (1994).

[34] H. Jarvelainen, P. Puolakkainen, S. Pakkanen *et al.*, "A role for decorin in cutaneous wound healing and angiogenesis," Wound Repair Regen, 14(4), 443-52 (2006).

[35] A. J. Schwartz, D. A. Wilson, K. G. Keegan *et al.*, "Factors regulating collagen synthesis and degradation during second-intention healing of wounds in the thoracic region and the distal aspect of the forelimb of horses," Am J Vet Res, 63(11), 1564-70 (2002).

[36] C. Antoniou, C. Dessinioti, D. Sotiriadis *et al.*, "A multicenter, randomized, split-face clinical trial evaluating the efficacy and safety of chromophore gel-assisted blue light phototherapy for the treatment of acne," Int J Dermatol, 55(12), 1321-1328 (2016).

[37] A. Nikolis, S. Fauverghe, G. Scapagnini *et al.*, "An extension of a multicenter, randomized, split-face clinical trial evaluating the efficacy and safety of chromophore gel-assisted blue light phototherapy for the treatment of acne," Int J Dermatol, 57(1), 94-103 (2018).

[38] R. A. Weiss, D. H. McDaniel, R. G. Geronemus *et al.*, "Clinical trial of a novel non-thermal LED array for reversal of photoaging: clinical, histologic, and surface profilometric results," Lasers Surg Med, 36(2), 85-91 (2005).

[39]   M. C. E. Nielsen, E. Devemy, J. Jaworska *et al.*, "Introducing: photobiomodulation by low energy chromophore-induced fluorescent light (Abstract)," SPIE BiOS, San Francisco, California, United States, (2017).

[40]   M. R. Hamblin, [Handbook of low-level light therapy] Pan Stanford Publishing, (2016).

[41]   K. Haltaufderhyde, R. N. Ozdeslik, N. L. Wicks *et al.*, "Opsin expression in human epidermal skin," Photochem Photobiol*, 91(1), 117-23 (2015).

[42]   A. Gupta, T. Dai, and M. R. Hamblin, "Effect of red and near-infrared wavelengths on low-level laser (light) therapy-induced healing of partial-thickness dermal abrasion in mice," Lasers Med Sci*, 29(1), 257-65 (2014).

[43]   I. Castellano-Pellicena, N. E. Uzunbajakava, C. Mignon *et al.*, "Does blue light restore human epidermal barrier function via activation of Opsin during cutaneous wound healing?," Lasers Surg Med, (2018).

[44]   S. Chifflet, C. Justet, J. A. Hernandez *et al.*, "Early and late calcium waves during wound healing in corneal endothelial cells," Wound Repair Regen*, 20(1), 28-37 (2012).

[45]   M. Greco, G. Guida, E. Perlino *et al.*, "Increase in RNA and protein synthesis by mitochondria irradiated with helium-neon laser," Biochem Biophys Res Commun*, 163(3), 1428-34 (1989).

[46]   T. I. Karu, and S. F. Kolyakov, "Exact action spectra for cellular responses relevant to phototherapy," Photomed Laser Surg*, 23(4), 355-61 (2005).

[47]   H. Liu, R. Colavitti, Rovira, II *et al.*, "Redox-dependent transcriptional regulation," Circ Res*, 97(10), 967-74 (2005).

[48]   P. V. Peplow, T. Y. Chung, B. Ryan *et al.*, "Laser photobiomodulation of gene expression and release of growth factors and cytokines from cells in culture: a review of human and animal studies," Photomed Laser Surg*, 29(5), 285-304 (2011).

[49]   J. van Horssen, P. van Schaik, and M. Witte, "Inflammation and mitochondrial dysfunction: A vicious circle in neurodegenerative disorders?," Neurosci Lett, (2017).

[50]   M. F. Alexeyev, S. P. Ledoux, and G. L. Wilson, "Mitochondrial DNA and aging," Clin Sci (Lond)*, 107(4), 355-64 (2004).

[51]   I. R. Lanza, and K. S. Nair, "Mitochondrial function as a determinant of life span," Pflugers Arch*, 459(2), 277-89 (2010).

[52]   E. L. Robb, M. M. Page, and J. A. Stuart, "Mitochondria, cellular stress resistance, somatic cell depletion and lifespan," Curr Aging Sci*, 2(1), 12-27 (2009).